



## Quasi-1D In/Si(111) Surface Structures

Andrey A. Stekolnikov, Xochitl López-Lozano,  
Jürgen Furthmüller, and Friedhem Bechstedt

published in

*NIC Symposium 2006*,  
G. Münster, D. Wolf, M. Kremer (Editors),  
John von Neumann Institute for Computing, Jülich,  
NIC Series, Vol. 32, ISBN 3-00-017351-X, pp. 143-150, 2006.

© 2006 by John von Neumann Institute for Computing

Permission to make digital or hard copies of portions of this work for personal or classroom use is granted provided that the copies are not made or distributed for profit or commercial advantage and that copies bear this notice and the full citation on the first page. To copy otherwise requires prior specific permission by the publisher mentioned above.

<http://www.fz-juelich.de/nic-series/volume32>

# Quasi-1D In/Si(111) Surface Structures

Andrey A. Stekolnikov<sup>1</sup>, Xochitl López-Lozano<sup>1,2</sup>,  
Jürgen Furthmüller<sup>1</sup>, and Friedhelm Bechstedt<sup>1</sup>

<sup>1</sup> Institut für Festkörpertheorie und -optik, Friedrich-Schiller-Universität  
Max-Wien-Platz 1, 07743 Jena, Germany  
*E-mail:* {andrey.furth, bech}@ifo.physik.uni-jena.de

<sup>2</sup> Instituto de Física, Universidad Autónoma de Puebla  
Apartado Postal J-48, Puebla 72570, México  
*E-mail:* xlopez@fisica.unam.mx

The atomic geometry and electronic structure is studied by means of *ab initio* total-energy and electronic-structure calculations for quasi-one-dimensional (1D) In/Si(111) systems with different translational symmetries  $4\times 1$ ,  $4\times 2$ , and  $8\times 2$ . The chain structure and the trimer formation are related to the details of the electronic band structure. While  $4\times 1$  reconstruction shows metallic behavior, the  $4\times 2$ , and  $8\times 2$  ones lead to an opening of energy gaps. We show that the phase transitions give rise to charge density waves in the electron density distribution. The electron redistributions are identified to play an important role for the transition  $4\times 2 \rightarrow 8\times 2$ . Only a weak tendency for spin ordering accompanying the surface reconstruction is found within the used spin-polarized density functional calculations.

## 1 Introduction

Adsorption of indium (In) on Si(111) substrates gives rise to a variety of surface reconstructions in dependence on the coverage with a tendency to be semiconducting below one monolayer or to be metallic at larger coverages. Most interesting is the borderline of these coverages for one monolayer for which a  $4\times 1$  phase occurs at room temperature (RT). Using grants of computational time by the John von Neumann Institute for Computing (NIC) we have performed highly demanding first-principle calculations in order to study atomic geometry, electronic band structure, and spin dependence of In chains on Si(111) substrates. We focus our attention to the interplay between the atomic structure of a given translational symmetry and the spatial distributions of charge, spin and electronic states. The results are discussed in terms of possibly occurring charge or spin density waves. The manifestation of charge density waves is studied in details. We try to extract driving forces for the reconstructions.

## 2 Motivation

True one-dimensional electronic systems have attracted great interest because of their expected exotic electronic properties, which include charge-density wave (CDW), spin-density wave (SDW), triplet superconductivity, and Luttinger-liquid (LL) behavior<sup>1</sup>. Properties of electrons related to charge and spin may be separated in a quasiparticle picture<sup>2</sup>. In a LL the electron loses its identity and separates into two quasiparticles. In a photoemission experiment the excitation should decay into a spinon that carries spin without charge and a holon that carries the positive charge of a hole without its spin. Metal chains of

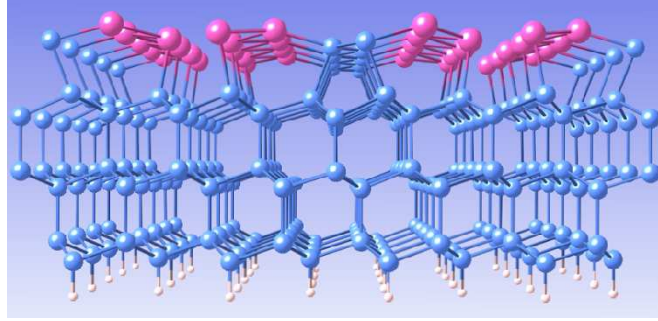


Figure 1. Side view of In/Si(111) system. The  $4 \times 1$  reconstruction is based on double zig-zag chain formation of In atoms.

clear 1D character should exhibit a Peierls instability<sup>3</sup> which results in a phase transition accompanied by a change in the translational symmetry. In quasi-1D metallic systems, electrons and holes near the Fermi energy often couple strongly with lattice vibrations, thereby generating a periodic spatial modulation of charge, i.e., a CDW which may open a band gap, a CDW gap<sup>1,4</sup>. Indeed, for the quasi-1D In/Si(111) system phase transitions have been observed. The  $4 \times 1$  arrangement of the In chains was found to undergo a reversible temperature-induced phase transition below 120K<sup>4,5</sup>. At a transition temperature of about 100K, a  $4 \times 2$  phase occurs that gradually changes over into a  $8 \times 2$  structure after further cooling<sup>4-6</sup>. The principle structure of In chains at 1 ML coverage is shown in Fig. 1. Whereas the generally accepted structural model of the RT  $4 \times 1$  structure<sup>7,8</sup> is able to explain well the majority of experimental observations, there are limitations<sup>6</sup> of the structural models proposed for the  $4 \times 2$  and  $8 \times 2$  reconstructions<sup>7,8</sup>. These models are based on the assumption that mainly the outer In atoms of the paired zigzag subchains of metal atoms should be affected by the reconstruction and not the inner In atoms. A tendency for pairing of the outermost chain atoms is accompanied by the formation of trimers<sup>5</sup>. However, the arrangement of the trimers is under debate<sup>9</sup>.

### 3 Method and Numerical Details

The total energies and the electronic structures are calculated within the density functional theory (DFT)<sup>10</sup> and the generalized gradient approximation (GGA)<sup>11</sup> for exchange and correlation. In the spin-polarized case the correlation energy for arbitrary polarization is determined by the same interpolation as for the exchange energy<sup>12</sup>. Explicitly we use the VASP code<sup>13</sup>. The electron-ion interaction is basically treated by non-norm-conserving ultrasoft pseudopotentials<sup>14</sup>.

The Si(111) surface is simulated by repeated asymmetric slabs with six Si bilayers and a vacuum region of the same extent<sup>15</sup>. The bottom side of each slab with fixed atomic positions is saturated by hydrogen atoms to simulate bulk Si. The addition of a half Si adlayer and a complete In monolayer allow us to model the quasi-1D In/Si(111) systems with  $4 \times 1$ ,  $4 \times 2$ , or  $8 \times 2$  translational symmetry.

The  $\mathbf{k}$ -space integrations for total energies and charge densities are done with a  $4 \times 8$  Monkhorst-Pack (MP) type mesh<sup>16</sup> (32  $\mathbf{k}$ -points) in the surface Brillouin zone (BZ) of the

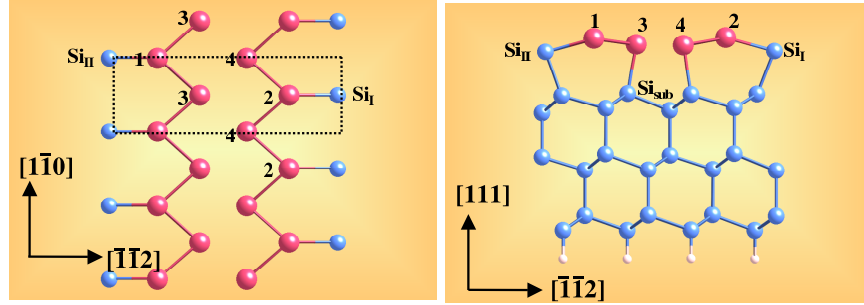


Figure 2. Top (left) and side (right) views on In/Si(111) surface with  $4 \times 1$  translational symmetry.

$4 \times 1$  structure. The number of  $\mathbf{k}$  points is correspondingly reduced for the larger surface unit cells,  $4 \times 2$  and  $8 \times 2$  ( $4 \times 4$  and  $2 \times 4$  MP type meshes). The atoms in the three lower bilayers are used to keep their bulk positions during the ionic relaxation. Using a variety of starting geometries representing a defined translational symmetry, several model structures have been tested and compared with respect to their total energy. The surface geometries are determined by relaxing the atomic positions until the Hellmann-Feynman forces are less than  $10 \text{ meV/\AA}$ .

## 4 Results

### 4.1 Atomic Geometry

In the case of a monolayer In coverage on a Si(111) substrate, the lowest total energies have been obtained for the chain model<sup>7,5</sup> in Fig. 2 representing the  $4 \times 1$  surface translational symmetry. Indium chains (wires) are composed of two zigzag rows (or subchains) parallel to the  $[\bar{1}10]$  direction. Below the In layer there are zigzag chains of Si atoms which separate the In nanowires in  $[11\bar{2}]$  direction. The arrangement of the Si atoms exhibits similarities with the reconstruction elements of the Si(111) $2 \times 1$  surface assuming the  $\pi$ -bonded chain model<sup>15,17</sup>. The In atoms at the chain edges (outermost or outer In atoms) are adsorbed at almost  $T_4$  and  $H_3$  adsorption sites of the Si(111) surface<sup>17</sup>. They lie higher than the In atoms in the interior of the chains, i.e., the In atoms belonging to adjacent subchains. These inner In atoms are adsorbed at on-top sites and, in turn, lie higher than the atoms in the Si chains. Mostly the actual arrangement of the outer In atoms determines the surface translational symmetry  $4 \times 1$  (Fig. 2),  $4 \times 2$  or  $8 \times 2$  (Fig. 3).

The overall structure of the In chains and their arrangement with respect to the Si atoms between the chains as well as the Si substrate atoms, agree well with the other first-principles calculations<sup>8,9,18-20</sup> as well as the data of x-ray diffraction<sup>7</sup> and low energy electron diffraction (LEED)<sup>21</sup>. The calculated In-In bond lengths in the two subchains of  $2.96\text{-}2.97 \text{ \AA}$  slightly overestimate the sum  $2.88 \text{ \AA}$  of two covalent radii ( $1.44 \text{ \AA}$ ) of In atoms, while the average distance  $3.12 \text{ \AA}$  of two In atoms in adjacent subchains comes closer to the nearest-neighbor value  $3.25 \text{ \AA}$  in a bulk In metal. The interatomic distances of the In chain atoms to the Si atoms in the trenches as well as in the substrate are only a little bit larger than the sum  $2.55 \text{ \AA}$  of the covalent radii of In ( $1.44 \text{ \AA}$ ) and Si ( $1.11 \text{ \AA}$ ). Our optimized structure shows excellent agreement with the LEED findings<sup>21</sup>. In principle, such

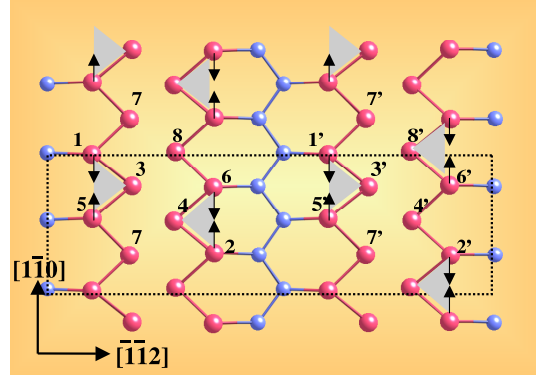


Figure 3. Top view of In/Si(111)  $8 \times 2$  ( $4 \times 2$ ) translational symmetry. In the case of  $4 \times 2$  reconstruction the trimers in different wires would be in phase. The pairing/trimer formation of In atoms is indicated by arrows.

a statement is also valid for the comparison with the SXRD data<sup>7</sup> and the other *ab-initio* calculations<sup>8,20</sup>. In the  $4 \times 2$  case we confirm that the outer In chain atoms are displaced by about 0.3 Å towards each other to form pairs and finally trimers with one of the inner chain atom (see Fig. 3). This movement gives rise to a doubling of the periodicity along the chains. As a result, two trimers (each in one subchain) belong to a  $4 \times 2$  unit cell. The remaining inner In atoms form less bonded pairs. A possible trimer arrangement (giving rise to the lowest total energy) is shown in Fig. 3. The energy gain of this reconstruction is small. We find that the  $4 \times 2$  geometry is more stable than the  $4 \times 1$  surface by about 3 meV per  $4 \times 1$  unit cell. In the  $8 \times 2$  case the trimer arrangement of Fig. 3 yields to a minimum on the total-energy surface with a rather small energy gain with respect to the  $4 \times 2$  geometry. Our  $8 \times 2$  structure gains 0.9 meV per  $4 \times 1$  unit cell with respect to the  $4 \times 2$  reconstruction.

## 4.2 Band Structure

The resulting electronic band structures are plotted in Fig. 3 versus high-symmetry lines in the BZs for the  $4 \times 1$  and  $4 \times 2$  reconstructed surfaces. The border lines of the irreducible part  $\Gamma XMY\Gamma$  and  $\Gamma X'M'Y'\Gamma$  of the two adopted rectangular BZs are chosen. The Fermi levels are calculated to be about 0.14 eV ( $4 \times 1$ ) or 0.13 eV ( $4 \times 2$ ) above the bulk valence band maximum for the two geometries. In the  $4 \times 1$  case the band structure in Fig. 3(a) clearly represents a metallic surface. One does not observe any surface states in the projected Si band gap along the  $\Gamma Y$  direction perpendicular to the chains. However, for the parallel direction  $XM$  at the BZ boundary four surface bands with weak dispersion are visible below the Fermi level. They show a stronger dispersion along the chains, i.e., along  $\Gamma X$  and  $MY$ . Three surface bands  $m_1$ ,  $m_2$ , and  $m_3$  cross the Fermi level and vary between the energetical regions of bulk valence and conduction bands. They are partially filled with 0.17 ( $m_1$ ), 0.83 ( $m_2$ ), and 1.00 ( $m_3$ ) electrons<sup>22</sup>. The described band-structure picture is in agreement with calculations<sup>8,23</sup> and PES/IPES measurements<sup>6</sup>.

The band structure of the In/Si(111) $4 \times 2$  surface in Fig. 3(b) cannot solely be explained in terms of folding of the  $4 \times 1$  bands due to the reduction of the BZ in the direction parallel to the chains. Rather, due to the discussed distortions of the geometry with respect to the

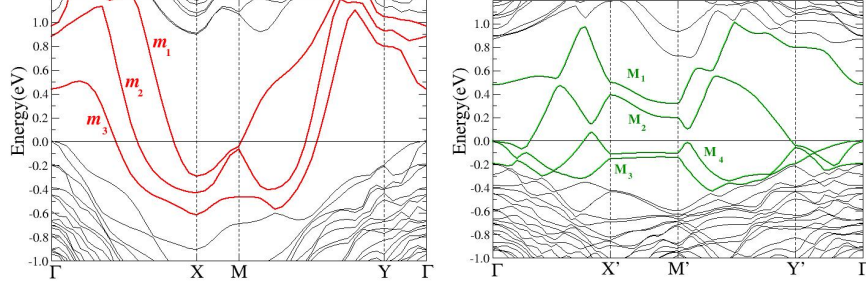


Figure 4. Electronic band structures of In/Si(111)(4 $\times$ 1) (a) and 4 $\times$ 2 (b) surfaces versus wave vectors along high symmetry lines parallel and perpendicular to the chains in the corresponding Brillouin zones. The horizontal lines define the Fermi levels. The adsorbate-related surface bands in the projected fundamental gap of Si are denoted by  $m_1$ ,  $m_2$ , and  $m_3$  (4 $\times$ 1) or  $M_1$ ,  $M_2$ ,  $M_3$ , and  $M_4$  (4 $\times$ 2).

4 $\times$ 1 surface, in particular the pairing mechanism, degeneracies of bands are lifted and at band-crossing points band repulsion occurs. One observes four new surface bands  $M_1$ ,  $M_2$ ,  $M_3$ , and  $M_4$  in the projected bulk fundamental gap which do not cross each other. These bands consist of folded branches of the former  $m_1$ ,  $m_2$ , and  $m_3$  bands, but their dispersion is remarkably modified by the opening of band gaps<sup>22</sup>. However, there is no opening of a true gap separating completely occupied and empty surface bands, so that the 4 $\times$ 2 surface with the geometry of Fig. 3 remains metallic.

### 4.3 Charge Density Waves

The changes of the band structures in Fig. 3 between the 4 $\times$ 1 and 4 $\times$ 2 geometries and the small variations of the total density of states are accompanied by a redistribution of the electrons in the surface region which may result in a CDW along the chains. In order to demonstrate this effect, in Fig. 5(a) we have plotted the difference of the total electron density of the 4 $\times$ 2 surface and the corresponding density for the 4 $\times$ 1 reconstruction in the area of a 4 $\times$ 2 unit cell. Figure 5(b) shows a similar contour plot for the 8 $\times$ 2 reconstruction with respect to the 4 $\times$ 1 surface.

The variations of the electron density in the 4 $\times$ 2 case relative to the 4 $\times$ 1 density clearly indicate the pairing mechanism as the driving force for the phase transition 4 $\times$ 1 $\rightarrow$ 4 $\times$ 2. Figure 5(a) shows an increase of the electron density in the region between two paired atoms in each subchain and an electron deficit in the adjacent regions. The probability to find electrons seems to be also increased in the regions of the Si-In bonds. In-In bonds become somewhat ionic in the 4 $\times$ 2 case. In addition, there is also an increase of electron density in the region between two adjacent trimers belonging to two different subchains. A deficit of electrons is obvious between two trimers in one subchain. The redistribution of electrons is similar in the 8 $\times$ 2 case.

Considering the situations in the two subchains separately, one may immediately interpret the phase transition 4 $\times$ 1 $\rightarrow$ 4 $\times$ 2 as well as 4 $\times$ 1 $\rightarrow$ 8 $\times$ 2 as the formation of a CDW (in each subchain). It seems that in Fig. 5(a) (i.e., for 4 $\times$ 2 surface) two CDWs of this kind are locked in during the temperature-induced phase transition. In the 8 $\times$ 2 case (Fig. 5(b)), more or less one CDW is locked in for each wire.

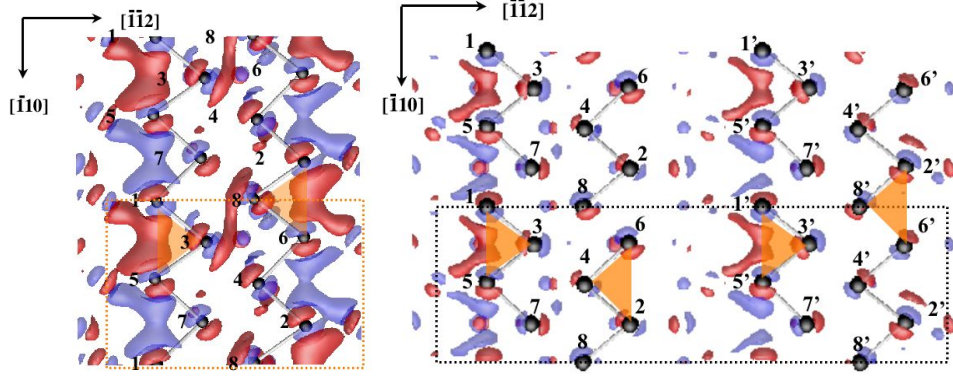


Figure 5. Difference of the total valence-electron densities of the  $4 \times 2$  and  $4 \times 1$  (a) or  $8 \times 2$  and  $4 \times 1$  (b) In/Si(111) surfaces. Red color indicates regions of electron excess, whereas blue color describes regions of electron depletion.

#### 4.4 Spin Density Waves

The question is if such a spinol-holon separation announced for 1D systems and a Luttinger liquid can also happen in a real quasi-1D system and lead to a spatial spin distribution different from the charge distribution. One may discuss the occurrence of a periodic modulation of the distribution of the electron spins along the chain direction. Therefore, similarly to the discussion of possible CDWs accompanying the phase transitions  $4 \times 1 \rightarrow 4 \times 2$  and  $4 \times 2 \rightarrow 8 \times 2$ , we ask the question whether a periodic spin arrangement may stabilize a certain surface reconstruction or not. For that reason we perform spin-polarized total energy calculations for a given atomic geometry but for different distributions of the electron spins over the In chain atoms in the nanowires on the  $4 \times 1$ -,  $4 \times 2$ - and  $8 \times 2$ -reconstructed In/Si(111) surfaces. Initial spin arrangements for  $4 \times 1$ -,  $4 \times 2$ - and  $8 \times 2$ - are shown in Fig. 6. They represent antiferromagnetic orderings with a vanishing total spin of the  $4 \times 1$ -,  $4 \times 2$ - and also  $8 \times 2$ - unit cell. We search for local minima on the total-energy surface with a finite magnetization density of the chain systems. The values of the initial local spins are varied until an energy minimum is reached. The resulting energies are compared with those obtained in the case without spin polarization.

The four initial configurations in the  $4 \times 1$  case represent arrangements of subchains with ferromagnetic (configurations 3 and 4) or antiferromagnetic (configurations 1 and 2) orderings, which may be displaced against each other. The total magnetic ordering in each complete wire is antiferromagnetic in all starting configurations. However, the optimization of the total energy leads to almost vanishing magnetic effects. Consequently, the accompanying energy gains are only of the order of 1 meV and the maximum splitting of the surface bands amounts to 6 meV for  $m_3$  near  $X$  and  $M$ . The same result is obtained for the first configuration in the  $4 \times 2$  case (Fig. 8(b)). The combination of two ferromagnetic subchains is not possible. The arrangement of antiferromagnetic subchains displaced by the vector against each other (configuration 2) gives rise to a slightly larger magnetization of  $0.02\mu_B$ . But still all accompanying effects are negligible. We conclude that a tendency for magnetic ordering within the In chains and, hence, the tendency for formation of SDWs is extremely small for the atomic geometries under consideration. There are practically no



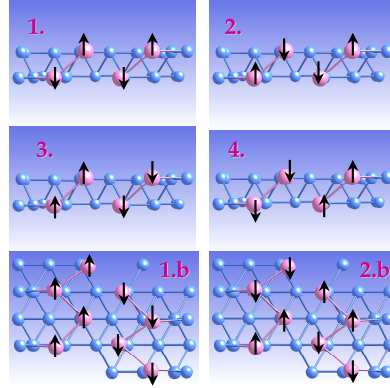


Figure 6. Initial spin configurations (top views) in the In chains of In/Si(111) with  $4\times 1$  (1-4) and  $4\times 2$  (1b, 2b) translational symmetry. Spin-up and spin-down are indicated by corresponding arrows.

additional driving forces for the studied reconstructions due to a certain antiferromagnetic ordering of the In atoms in the quantum wires.

## 5 Concluding Remarks

In summary, the atomic, electronic, and spin structures of arrays of quasi-1D indium chains on Si(111) substrates have been investigated by *ab initio* density-functional theory calculations. In the case of the room-temperature  $4\times 1$  surface structure, excellent agreement has been found with experimental results and results of other *ab-initio* calculations for the atomic structure and the band structure. We agree with recent x-ray diffractions measurements and total-energy optimizations that pairing of In atoms in the subchains and the accompanying formation of trimers is the basic mechanism of the observed temperature-induced surface phase transitions  $4\times 1 \rightarrow 4\times 2$  and  $4\times 2 \rightarrow 8\times 2$  between different surface reconstructions. The geometric distortion due to the pairing gives rise to gap openings near band crossings along chain directions. However, despite the opening of gaps in the surface band structure, there are still two bands which keep a metallic character of the surface, although with a reduced density of the free carriers. The comparison of the electron densities of the  $4\times 1$  and  $4\times 2$  surfaces clearly indicates the formation and the lock-in of phase-shifted charge density waves in each subchains. According to the simulated electron excess and deficit regions, the phase transition  $4\times 2 \rightarrow 8\times 2$  should not be traced back to a CDW mechanism. Rather, the large distances of the chains of about 11 Å and the formation of a weak effective 2D ionic lattice due to the In-In pairing suggest long-range electrostatic forces as driving forces for the phase transition. The total-energy calculations with inclusion of the spin polarization clearly showed that practically there are not tendencies for magnetic orderings by antiferromagnetic spin arrangements and spin density waves. We conclude that modulations of the spin density do not contribute to a stabilization of neither the room-temperature nor the low-temperature phases of the In/Si(111) surface.

We have to mention that recently another hexagon-based  $4\times 2$  reconstruction geometry has been proposed<sup>9</sup>. Its band structure indicates a nonmetal but its energetical stability is under discussion<sup>24</sup>.



## Acknowledgments

We gratefully acknowledge a grant of supercomputer time provided by the NIC Jülich. We acknowledge financial support from the Deutsche Forschungsgemeinschaft (Project Nos. Be 1346/16-1), the European Community in the framework of the NoE NANOQUANTA (NMP4-CT-2004-500198).

## References

1. G. Grüner, *Density Waves in Solids* (Addison-Wesley, Reading, MA 1994).
2. J.M. Luttinger, J. Math. Phys. (N.Y.) **4**, 1154 (1963).
3. R.E. Peierls, *Quantum Theory of Solids* (Clarendon, Oxford, 1964).
4. H.W. Yeom, S. Takeda, E. Rotenberg, I. Matsuda, K. Horikoshi, J. Schaefer, C.M. Lee, S.D. Kevan, T. Ohta, T. Nagao, and S. Hasegawa, Phys. Rev. Lett. **82**, 4898 (1999).
5. C. Kumpf, O. Bunk, J.H. Zeysing, Y. Su, M. Nielsen, R.L. Johnson, R. Feidenhans'l, and K. Bechgaard, Phys. Rev. Lett. **85**, 4916 (2000).
6. H.W. Yeom, K. Horikoshi, H.M. Zhang, K. Ono, and R.I.G. Uhrberg, Phys. Rev. B **65**, 241307(R) (2002).
7. O. Bunk, G. Falkenberg, J.H. Zeysing, L. Lottermoser, R.L. Johnson, M. Nielsen, F. Berg-Rasmussen, J. Baker, and R. Feidenhans'l, Phys. Rev. B **59**, 12228 (1999).
8. J.-H. Cho, J.-Y. Lee and L. Kleinman, Phys. Rev. B **71**, 081310(R) (2005).
9. C. González, J. Ortega and F. Flores, New Journal of Physics **7**, 100 (2005).
10. P. Hohenberg and W. Kohn, Phys. Rev. **136**, B864 (1964); W. Kohn and L.J. Sham, Phys. Rev. **140**, A1133 (1965).
11. J.P. Perdew, in *Electronic Structure of Solids '91*, edited by P. Ziesche and H. Eschrig (Akademie-Verlag, Berlin, 1991), p. 11.
12. U. von Barth and L. Hedin, J. Phys. C **5**, 1629 (1972).
13. G. Kresse and J. Furthmüller, Comput. Mater. Sci. **6**, 15 (1996); Phys. Rev. B **54**, 11169 (1996).
14. J. Furthmüller, P. Käckell, F. Bechstedt, and G. Kresse, Phys. Rev. B **61**, 4576 (2000).
15. A.A. Stekolnikov, J. Furthmüller, and F. Bechstedt, Phys. Rev. B **65**, 115318 (2002).
16. H.J. Monkhorst and J.D. Pack, Phys. Rev. B **13**, 5188 (1976).
17. F. Bechstedt, *Principles of Surface Physics* (Springer, Berlin 2003).
18. J. Nakamura, S. Watanabe, and M. Aono, Phys. Rev. B **63**, 193307 (2001).
19. R.H. Miwa and G.P. Srivastava, Surf. Sci. **473**, 123 (2001).
20. S.-F. Tsay, Physical Review B **71**, 035207 (2005).
21. S. Mizuno, Y.O. Mizuno, and H. Tochiara, Phys. Rev. B **67**, 195410 (2003).
22. X. López-Lozano, A.A. Stekolnikov, J. Furthmüller, and F. Bechstedt, Surf. Sci. **589**, 77 (2005).
23. F. Bechstedt, A. Krivosheeva, J. Furthmüller, and A.A. Stekolnikov, Phys. Rev. B **68**, 193406 (2003).
24. A.A. Stekolnikov *et al.*, unpublished.